Materials Transactions, Vol. 44, No. 5 (2003) pp. 893 to 900
Special Issue on Solidification Science and Processing for Advanced Materials

Processing of Semi-Solid Gray Cast Iron Using the Cooling Plate Technique

Alex Muumbo*, Mitsuharu Takita and Hiroyuki Nomura

Department of Materials Processing Engineering, Nagoya University, Nagoya 464-8603, Japan

A semi-solid processing technique combining a cooling plate and various mold materials is developed to produce high quality gray cast iron components. Flow behavior of semi-solid slurry along an inclined cooling plate is studied to establish the effect of plate orientation on the integrity of cast products. The concept of multiple-stage cooling is discussed by considering cooling rates at different stages of processing along the cooling plate and in sand, graphite and metallic molds to show the significance of cooling rate in determining component microstructure. The morphology of microstructure in cast components is discussed and image analysis results presented. A refined microstructure of primary austenite and graphite, and their characteristics associated with the use of different mold materials are reported. Angle of inclination of plate is shown to influence the morphology and quantity of precipitated phases. Finally, the effects of cooling plate and mold material on Vickers hardness and mechanical strength of cast components are discussed.

(Received November 5, 2002; Accepted January 6, 2003)

Keywords: *semi-solid processing, cooling plate, crystal separation, melt-flow, gray cast iron, microstructure, primary austenite particles, graphite, tensile strength, fracture surface, Vicker's hardness*

1. Introduction

Recent attempts to make parts using semi-solid processing have proved beneficial in terms of energy savings, and have resulted in improved quality of products. Initial work done by Qui[1] at Nagoya University investigated the thixotropic nature, primary particle/liquid segregation and mold-filling ability of mechanically stirred gray cast iron. The work showed that despite the high processing temperature, semi-solid gray cast iron behaves in manner similar to that exhibited by low temperature melting point alloys in the semi-solid state. Among proven techniques, mechanical stirring has been employed to prepare semi-solid slurries for a wide range of alloys[2–4] while electro-magnetic stirring[5,6] and the cooling plate[7] have been used to prepare slurries from alloys of aluminum and magnesium characterized by low melting points.

The suitability of the cooling plate in processing gray cast iron semi-solid slurry has however, so far not been fully investigated. This paper aims to clarify the effect of the cooling plate on flow behavior of gray cast iron slurry and its influence on the kinetics of nucleation of both primary austenite and graphite as explained by crystal separation theory.[7–10] The process hinges on the refinement of primary grains and precipitated carbon through combined rapid solidification and flow-related fragmentation of dendrites to form a globular structure, enhancing the mechanical properties of cast products. In this process, equiaxed microstructure evolves from crystals that nucleate on the plate wall having the growth of their roots restricted by segregation of the solute. The crystals then separate before forming a stable solid shell and join the mainstream melt.[11] In situations where careful control of pouring temperature is maintained, besides reducing the grain size, convective forces acting upon the slurry along the cooling plate could minimize segregation of constituent elements resulting in improved mechanical properties.

*Graduate Student, Nagoya University. Corresponding author: E-mail: alex@eagle.numse.nagoya-u.ac.jp

2. Experimental Method

In the present study, an electric resistance furnace is used to prepare melt samples weighing approximately 700 g. The charge is heated in an argon atmosphere up to a temperature of 1723 K then soaked for one hour to ensure complete melting, followed by cooling in the furnace for 30 minutes to allow the charge attain the desired temperature. The argon atmosphere helps keep the melt composition shown in Table 1 by minimizing decarburization and oxidation effects. At the desired temperature just above the liquidus, the melt charge is removed from the furnace and poured over a cooling plate inclined at a known angle to the horizontal as illustrated in Fig. 1, and allowed to flow into a mold with a cavity of known dimensions at the end of the inclined plate. Simultaneously temperature readings are taken using thermocouples connected to a data logger set to record data at 100 millisecond intervals.

Before pouring, a boron nitride coating is applied on the surface of the cooling plate to allow precipitating crystals to separate easily from the cooling plate wall. Three types of mold materials; sand, graphite and steel are used in the casting experiments. A graphite/boron nitride coating is also applied onto the cavity wall of the metallic mold to improve melt feeding and provide a thermal cushion to the mold material. Upon cooling, cast components are extracted from the molds and samples prepared for Vickers hardness, tensile tests and microstructure examination.

Table 1 Cast iron sample composition. (mass%)

Sample	C	Si	Mn	P	S	T_l/K	T_E/K	CE
1	2.87	2.01	0.48	0.02	0.09	1537	1407	3.54
2	3.17	2.20	0.48	0.02	0.09	1518	1410	3.88
3	3.20	2.10	0.50	0.09	0.09	1536	1383	3.93
4	3.30	2.11	0.02	0.49	0.11	1518	1393	4.00

T_L-Liquidus temperature, T_E-Eutectic temperature, CE = %C+1/3(%Si+%P).

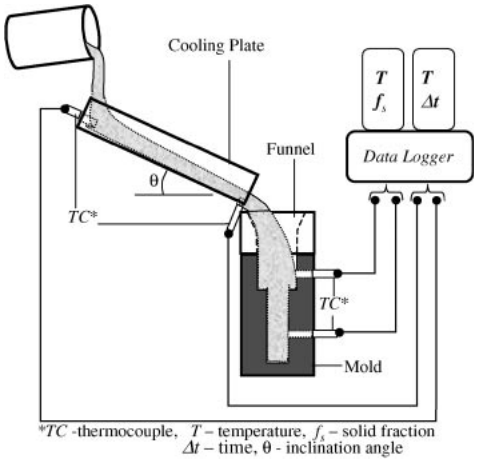

Fig. 1 Experimental set-up.

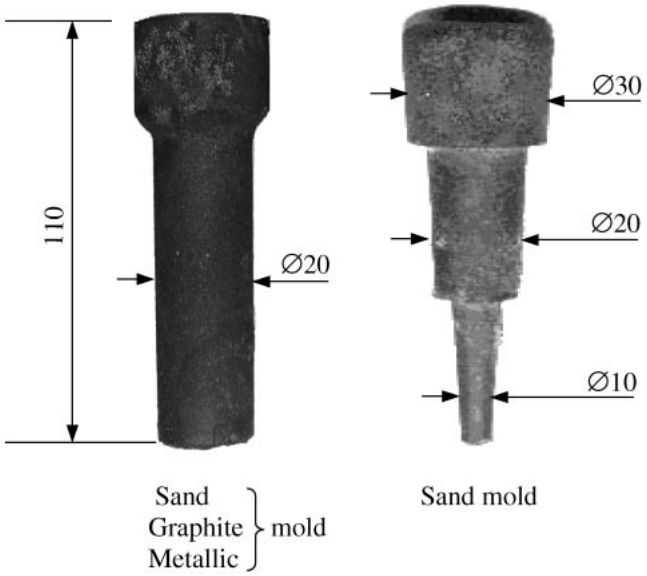

Fig. 2 Cast components.

3. Results and Discussion

3.1 Slurry flow velocity

When molten gray cast iron flows along an inclined *cooling plate*, cooling rates as high as 67 K/s are obtained owing to heat-loss through the plate-wall. Under this condition, nucleation is initiated along the melt/plate contact surface and the melt-flow action draws nucleated crystals into the melt stream before they come into contact with adjacent crystals to form a solid shell. Nucleation and growth of primary phase taking place in the semi-solid state is influenced by the degree of undercooling, amount of nucleating agents, flow field and the rate of fragmentation of primary particle dendrite arms.[10] Temperature of the molten metal is normally lower near the plate wall and along the free surface due to conduction and radiation effects respectively. Convection arising from flow provides a mechanism for dissipation of superheat and detachment of nuclei from the plate wall.

Tests done using sample No. 3 in Table 1 show that low flow velocity encountered at low inclination angles causes early solidification of metal along the cooling plate, while excessive turbulence at high inclination angles, increases the likelihood of gas entrapment within the mold cavity. By varying the melt temperature and plate inclination angle between 5° and 15°, significant changes in components' external and internal structure are observed. Based on preliminary results, a combination of angle of 10° and a pouring temperature of 20 K above liquidus are adopted for the casting experiments.

3.2 Cast components

Two types of cast components are made by sand casting; one is straight cylindrical shape 20 mm in diameter, and another stepped cylindrical shape of dimensions shown in Fig. 2. For the metallic and graphite mold casting, straight cylindrical components 20 mm in diameter are cast.

3.3 Temperature measurements

Temperature measurements are made along the length of the cooling plate and at the entrance of mold cavity. Cooling pattern can be categorized into three distinct stages; Stage1-occurring along the cooling plate, Stage2-between the time just after the slurry enters the mold and immediately after eutectic solidification and Stage3-immediately after stage2 and up to a temperature just below the eutectoid. Figures 3(a) and (b) illustrate in-mold temperature profiles for three mold materials used and calculated cooling rates at the different stages respectively. Based on averages calculated from a number of experiments, the cooling rate over stage2 is highest for graphite mold at 6.3 K/s, while metallic and sand molds achieve 4.5 K/s, and 3.5 K/s respectively.

A high cooling rate during stage2 is considered to suppress the growth of precipitated primary particles while increasing the nucleation of graphite. During stage3 when solidification is complete, further cooling reaches the eutectoid temperature whereupon austenite transforms into pearlite or ferrite grains, their relative amounts being largely determined by chemical composition, cooling rate during decomposition and the nature of graphite structure.[12] Cooling rate during this stage also affects the eutectic cell morphology. The average cooling rates recorded for metallic, sand and graphite molds during stage3 are 3.0 K/s, 1.7 K/s and 1.2 K/s respectively.

3.4 Microstructure

Figure 4 shows unetched and etched microstructure from samples 1, 2 and 4, taken using an optical microscope for the experiments conducted at an inclination angle of 10° and pouring temperature 20 K above liquidus of the respective alloy compositions. The combined effect of cooling plate and mold material on microstructure of cast components is evident. Under normal casting, Fe–C–Si alloys of eutectic or near eutectic composition usually yield gray iron, having ferritic-pearlitic matrix structures and graphite in the form of flakes, in which layers of graphite basal planes are stacked together to form sheets.[13] During solidification, the first solid phase to form is primary austenite followed by one or a combination of the two eutectic phases. Under such circumstances, the morphology of gray iron microstructure is

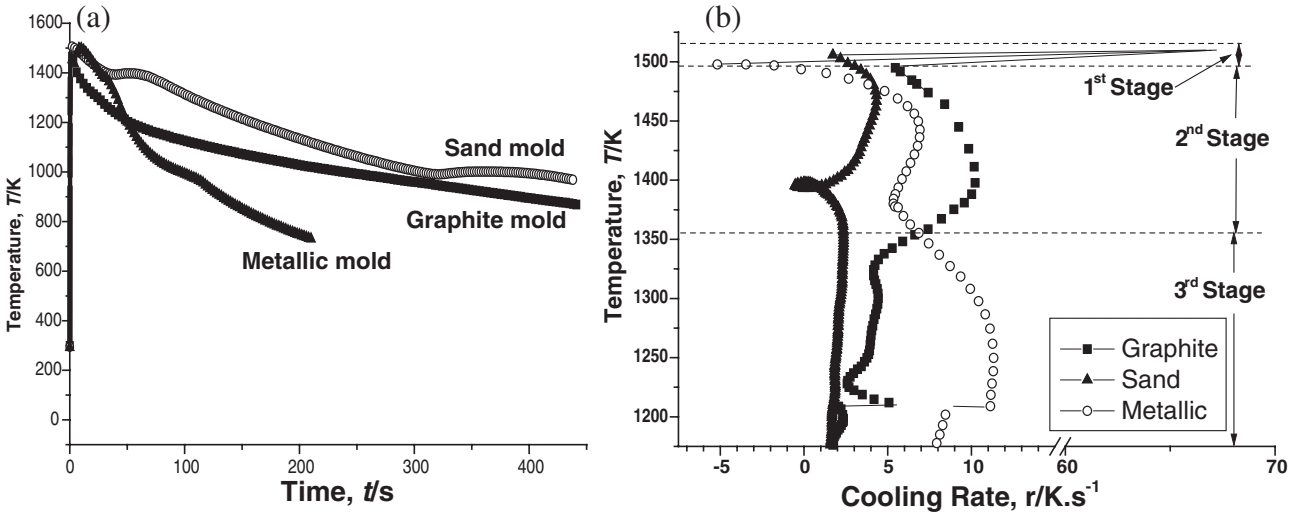

Fig. 3 (a) In-mold temperature profiles vs time. (b) Cooling rate vs temperature at different stages of processing.

determined by the cooling rate, composition, nucleation, and growth conditions prevailing during solidification and the transformation behavior of austenite during cooling through the critical temperature range.[14,15] Depending on the cooling rate, the austenite matrix can transform into pearlite or ferrite. With sufficient silicon as in the cases studied here, solidification may result in either austenite-graphite eutectic during slow cooling as observed in the sand and graphite mold castings, or austenite-carbide eutectic during rapid cooling, as seen in metallic mold castings. Between the equilibrium graphite temperature and the Fe–Fe_3C eutectic temperature, only the graphite eutectic may nucleate and grow depending on the undercooling.

In the case of semi-solid processing using the cooling plate, much of the primary graphite precipitates in granular form while secondary graphite phase precipitates within the eutectic grain in a flaky form. High undercooling below the metastable eutectic temperature promotes nucleation and growth of the Fe–Fe_3C eutectic, explaining why the Fe–Fe_3C eutectic is prevalent in the metallic mold casting than in the graphite or sand casting. For the metallic mold case, initiation of eutectic solidification promotes radial growth of the eutectic cell, clearly distinguishable from the graphite and primary austenite phases.

The cooling plate has distinct refining effect on primary austenite, graphite and the substructure. Experiments conducted show a strong influence of convection on grain size of cast metals. When convection is reduced, grain size becomes larger and columnar structures are more readily obtained. Depending on the mold material used, further changes in microstructure take place in the mold. Unetched samples show that normal sand castings largely possess a dendritic network of the primary phase, irrespective of composition. The enhanced growth of dendritic grains promotes precipitation of flaky graphite within the eutectic phase and along the grain boundaries as seen from the etched sample micrographs in Fig. 4.

The grains in normal castings have long uninterrupted surfaces which could be favored locations for collection of impurities that concentrate in the late solidifying liquid. For castings made using the cooling plate, irrespective of the mold material, a structure of well-defined eutectic grains is observable. Each eutectic cell shows an intricate formation of transformed austenite phase and graphite with a structure that appears branched and interconnected. The fineness of eutectic grains is largely determined by local interface velocity, which in this case is varied using different mold materials. In addition as pointed out by Flemings,[16] in eutectics of multicomponent alloys, local interface velocity is not determined by the rate of heat extraction alone but that it is also an inverse function of the number of grains from which solidification is proceeding in a local region.

Products made using the cooling plate show a more refined primary phase structure, whose size is dependent on the mold material employed. Despite the fact that solid-state transformations take place and which depending on the cooling rate in the mold could have a significant effect on the morphology of microstructure, in the case discussed here, formation of initial primary globular structure largely takes place when cooling within the semi-solid region. Depending on the mold material used, the average size of primary particles in microstructure produced using the cooling plate is about 50 μm in diameter which is smaller than that obtained with mechanical stirring, on an average 150 μm in diameter.[1]

3.5 Image analysis

Image analyses performed on optical micrographs show the size of eutectic grains varying with mold material, on average measuring 450 μm, 200 μm and 150 μm in radius for sand, metallic and graphite molds respectively.[17]

The effect of inclination angle on microstructure investigated by pouring melt down the cooling plate at angles between 5° and 15° is shown in Fig. 5. Graphite grain-count increases with increasing angle of inclination for graphite and metallic mold castings from 5° to 10° but decreases with subsequent increase in angle above 10°.

In Fig. 6, both the size and area ratio of the primary particles for the metallic mold castings show a slight decrease initially followed by a steep increase at higher angles. Growth of primary particles is partly due to carbon diffusion

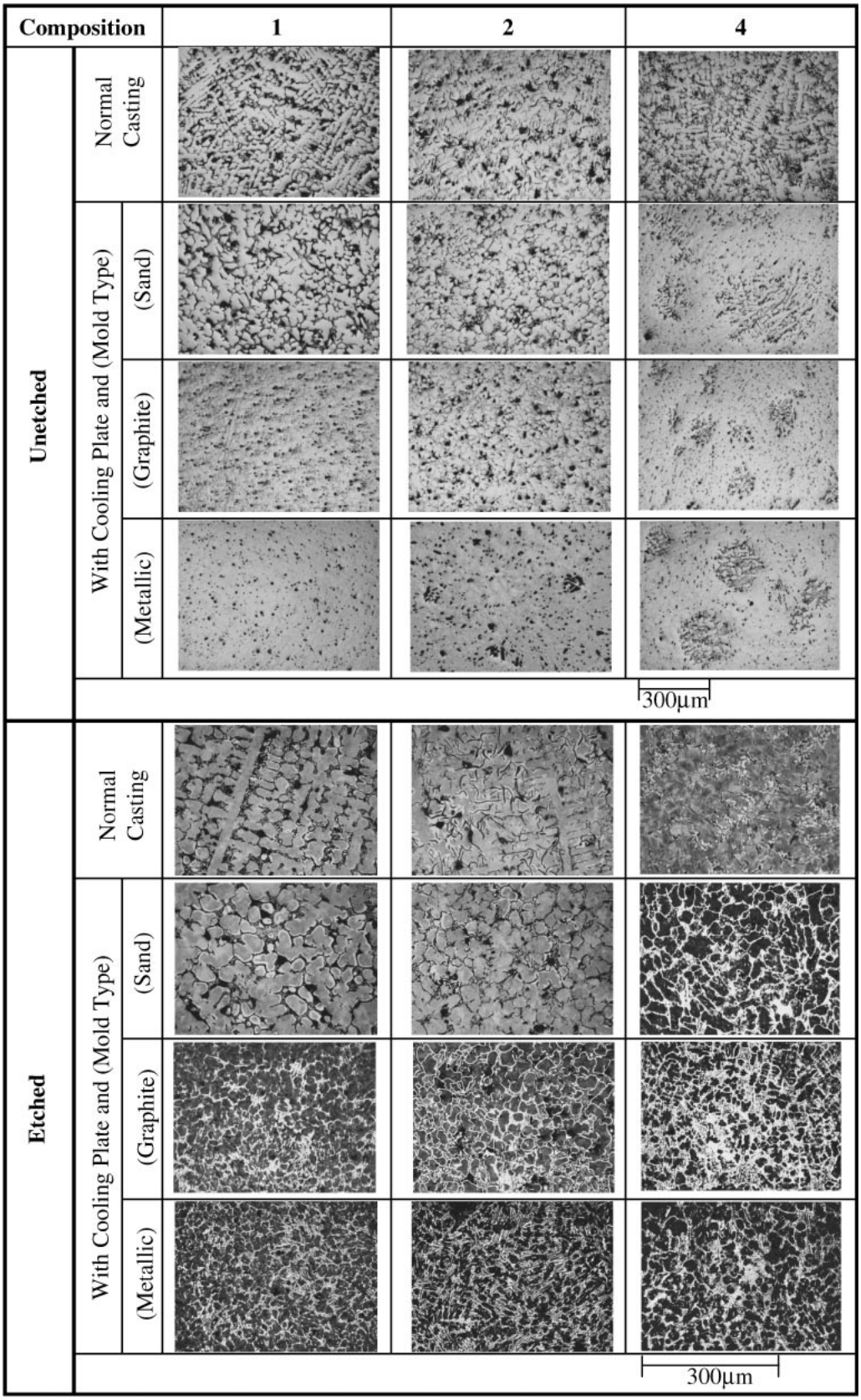

Fig. 4 Unetched and etched microstructure of components made under different experimental conditions.

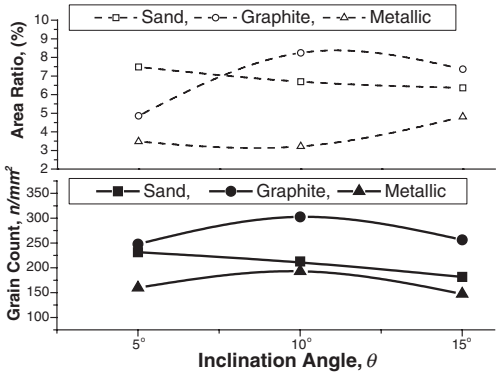

Fig. 5 Graphite grain count and average grain area ratio as a function of angle of inclination.

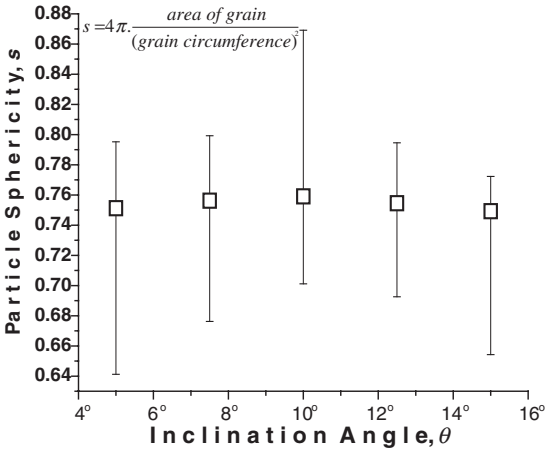

Fig. 7 Primary particle sphericity as a function of inclination angle.

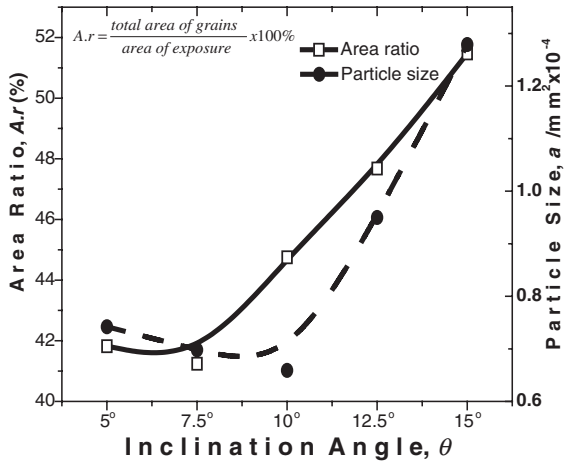

Fig. 6 Primary particle area ratio and particle size as a function of inclination angle.

and partly due to melt undercooling and supersaturation.[18] Increasing the angle of inclination increases the velocity of flow therefore reducing the time over which the slurry would be in contact with the cooling plate. As a result, slurry at the end of the cooling plate tends to have a higher fraction of liquid phase when filling the mold. This promotes the growth of primary particles, which could be the reason behind the observed (increasing) pattern.

The relationship between primary particle sphericity and inclination angle in samples of metallic mold casting is illustrated in Fig. 7. Generally, a high sphericity is obtained but appears to be slightly influenced by the inclination angle of the cooling plate. From Figs. 5 and 7, it can be deduced that graphite grain count and primary particle sphericity are highest for a combination of inclination angle of 10° and a pouring temperature 20 K above the liquidus, particularly for graphite and metallic mold cases respectively.

3.6 Fracture surface

Figure 8 shows SEM and Laser micrographs of fracture surfaces for the samples cast from melt batch 4 in Table 1. The micrographs reveal inter-granular fracture profile and general fracture surface respectively. Normal casting in sand molds produces a rough fracture surface owing to the coarse primary phase dendrites characterized by less-sharp peaks and the coarse/flaky structure of graphite. Combination of sand casting and cooling plate produces a finer grain structure, which under local stretching produces relatively longer and sharper peaks along the fracture surface. For graphite mold casting, the fracture surface exhibits extensive local stretching with intermittent flat areas signifying high content of graphite phase. For the sand and graphite casting, fracture is largely ductile, and tends to follow grain boundaries, exposing graphite nodules that are occasionally pulled away from the metal in local phase boundary fracture, leaving deep spherical cavities visible in the micrographs.

For the metal mold casting, a largely unidirectional brittle fracture mode is evident. The matrix shows a tendency to cleave along pearlite-cementite interfaces within the eutectic matrix. This yields a much smoother fracture surface compared with samples made in sand and graphite molds. From visual examination, the fracture surface for metallic mold castings appears white, while dark globular spots are visible against a gray background on the fracture surfaces of both the sand and graphite castings. Coarseness of structure for sand castings appears to lie between that for metallic and graphite mold castings. Generally, both primary interfacial (*i.e.* graphite/metal interface) fractures and secondary interfacial (*i.e.* inter-crystalline graphite interface) fractures are observed. Fracture mode appears to be largely influenced by the growth of crystals along preferred crystallographic directions.

3.7 Mechanical properties

3.7.1 Tensile strength

Room-temperature mechanical properties of cast structures are generally found to increase with decreasing grain size. The effects of grain size on the properties appear to result primarily from changes in the distribution of porosity, inclusions and micro-segregation.[19] The heterogeneities are particularly severe at grain boundaries and the preferred fracture paths present in coarse-grained structures result in lower mechanical properties. Under stress conditions, crack propagation through a microstructure of cast iron having flake graphite can occur relatively easily due to the almost continuous brittle graphite phase. Leube and Anberge[20] observe that increasing the fraction of primary dendrites

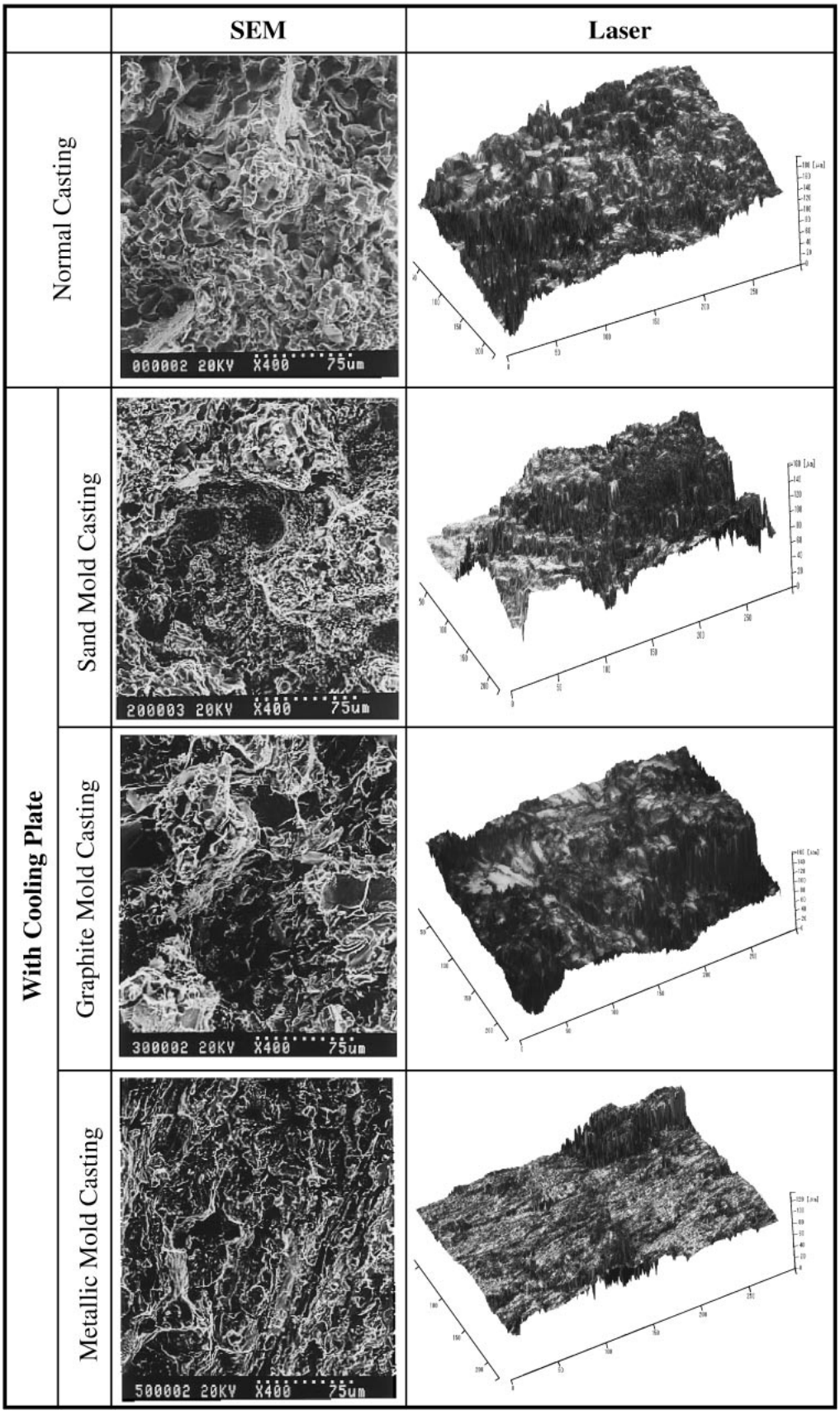

Fig. 8 Fracture surface for samples of composition 4 cast using different molds.

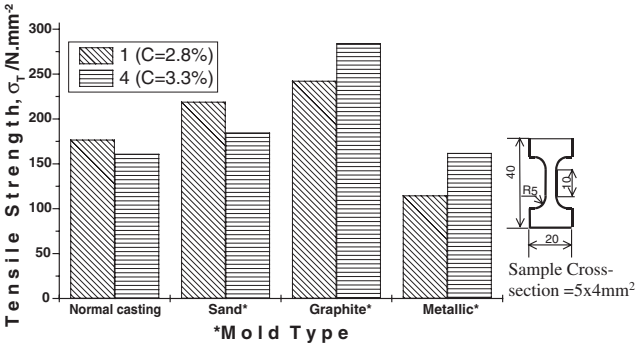

Fig. 9 Tensile strength as a function of mold material for compositions 1 and 4.

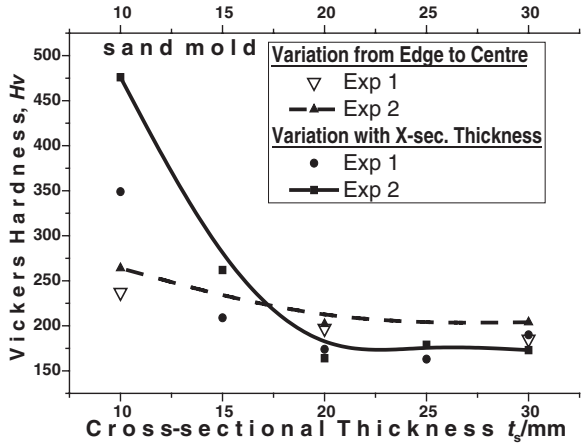

Fig. 11 Vicker's hardness as a function of cross-sectional thickness for sand mold castings.

while decreasing fraction of flaky graphite leads to higher tensile strength in normal gray cast iron. In contrast, the globularizing effect by the cooling plate on primary particle and graphite phases impedes local crack propagation in a sample under stress since globular particles are more difficult to fracture than flakes, and a crack cannot follow a semi-continuous path of graphite. As a result, the strength of samples made using the cooling plate is higher than that for normal casting as shown in Fig. 9.

The formation of a carbide eutectic or white iron is usually considered to be detrimental to gray iron castings because of its high hardness and low toughness. The relatively low strength obtained by metallic mold is considered to be due to the above reason. Ruff and Wallace[21] report that both fracture toughness and tensile strength of cast iron decreases linearly with increasing eutectic cell size. Results on tensile strength obtained by the authors also confirm the above.[17]

3.7.2 Hardness

Hardness values with respect to radial distance from the edge of specimens to the center are shown in Fig. 10 for cylindrical castings of 10 mm radius. Normal sand casting shows highest variability in comparison to specimens made through the cooling plate technique. Among these, the metallic mold posts highest hardness values while the sand mold posts the lowest. The phenomenon is thought to arise from differences in phases precipitated, their ratio and size. On average, the metallic mold sample has the lowest ratio of the graphite phase, followed by sand and graphite mold samples in increasing order. In addition, the white surface appearance observed on the surface of fractured metallic mold specimens signifies a higher fraction of carbide in the eutectic phase. The initially high cooling rate experienced in the graphite mold imparts higher hardness along the edge of the sample compared to the center where hardness approaches that for sand mold castings.

Tests performed on step-shaped cylindrical specimens of sand casting with radii varying between 10 and 30 mm yield the results shown in Fig. 11. Hardness generally decreases with increase in section-thickness of castings, but with minimal variation in the radial direction. For sections under 20 mm, hardness values increase sharply, to values almost equivalent to those recorded for castings made using the metallic mold.

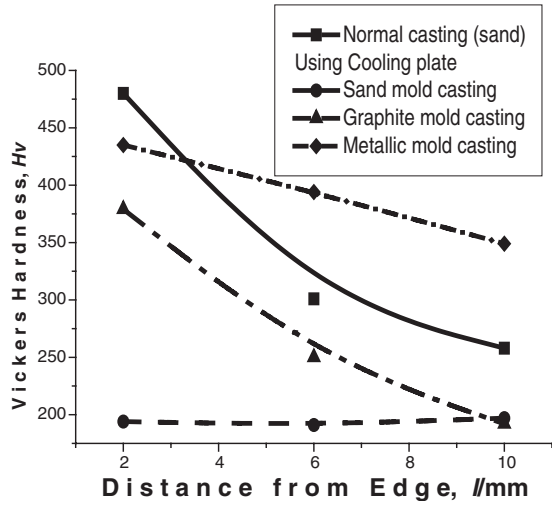

Fig. 10 Vicker's hardness as a function of radial distance.

4. Conclusions

Semi-solid processed cast iron is obtained by the use of cooling plate technique and its properties investigated for three mold materials.

(1) Turbulent flow over an inclined plate with boron nitride coating causes fragmentation of primary solidified phase, distributing the resulting particles uniformly within the melt stream.

(2) External and internal integrity of the components is influenced by inclination angle of the cooling plate and pouring temperature. Experiments carried out at 10 degrees inclination produce more structurally sound components than for other angles considered.

(3) Though in practice low pouring temperature is necessary for effective nucleation and globularization of the primary phase, with decreasing pouring temperature the flow of slurry down the cooling plate worsens considerably. Improvement of macro- and micro-structural characteristics of the products could be achieved through controlled pouring, ensuring constant initial temperature and plate surface condition. Heat transfer characteristics for semi-solid metal/cooling plate and

mold greatly affect the size and shape of resulting primary particles, and nature of the eutectic phase.

(4) Improvement of tensile strength in the present investigation is achieved by increasing the area-fraction of primary particles and refining of the eutectic cell size. Reduced tensile strength is observed in cases where the rate of cooling is low and also where carbides solidify in a unidirectional pattern.

(5) Highest and lowest hardness values are obtained with metallic mold castings and sand mold castings respectively. For sand castings, hardness varies with respect to section thickness, however, for same section thickness, uniform mechanical properties can be achieved.

REFERENCES

1) P. Qiu: PhD. *Thesis on Processing of semi-solid cast iron*, Nagoya Univ. Dept. of Mats. Proc. Eng. (2000).
2) P. Qiu, H. Nomura, M. Takita and M. Imaizumi: J. Japan Foundry Engineering. **71** (1999) 685–690.
3) M. Imaizumi, H. Nomura and M. Takita: *2nd Int. Conf. on Processing Materials for Properties*, (2000) pp. 1033–1036.
4) D. Brabazon, D. J. Browne and A. J. Carr: Mater. Sci. Eng. A **326** (2002) 370–381.
5) P. Kapranos, P. J. Ward, H. V. Atkinson and D. H. Kirkwood: Mater. Design. **21** (2000) 387–394.
6) Q. Wang, T. Momiyama, K. Iwai and S. Asai: Mater. Trans., JIM **41** (2000) 1034–1039.
7) A. Ohno, T. Motegi and H. Soda: Trans. ISIJ **11** (1971) 18–26.
8) J. Xing, T. Motegi and A.: Trans. JIM **26** (1985) 144–151.
9) T. Motegi and A. Ohno: Trans. JIM **25** (1984) 122–132.
10) A. Ohno and T. Motegi: AFS International Cast Metals Journal, Vol. (1977) 28–36.
11) A. Ohno: *Solidification, the separation theory and its applications*, Translated by; J. Wakabayashi, (Springer-Verlag 1987) 6–10.
12) D. D. Goettsch and J. A. Dantzig: Metall. Mater. Trans. **25A** (1994) 1063–1079.
13) J. Prwas and N. Mardesich: *Microstructural Science*, **6** (Proc 10th annual tech. meeting of the int. metallographic soc.-Elsevier 1977) 161–180.
14) J. F. Wallace: Trans. Am. Foundrymen's Soc. **88** (1975) 363–378.
15) D. Maijer, S. L. Cockroft and W. Patt: Metall. Trans. **30A** (1999) 2147–2157.
16) M. C. Flemings: *Solidification processing*, (McGrawhill Book Company, 1974) p. 154.
17) A. Muumbo, H. Nomura and M. Takita: 7th SPCI Conf. Barcelona Spain, (Sept. 2002).
18) S. Chang, D. Shanguan and D. Stefanescu: Metall. Trans. **23A** (1992) 1333-47.
19) M. C. Flemings: *Solidification Processing, Materials Science and Technology Series*-Processing of Metals and Alloys 15th Ed. by R. W. Cahn, P. Haasen and E. J. Krammer, (McGrawhill, Inc. 1991) 20–24.
20) B. Leube and L. Anberg: Int. J. of Cast Metals Research. **11** (1999) 507–514.
21) G. F. Ruff and J. F. Wallace: Trans. Am. Foundrymen's Soc. **56B** (1977) 179–202.